The Effect of Specific Nucleation on Molecular and Supermolecular Orientation in Isotactic Polypropylene

Jaroslav Ščudla[1], Klaus-Jochen Eichhorn[2], Miroslav Raab[1], Pavel Schmidt[1], Dieter Jehnichen[2], and Liane Häußler[2]

[1]Institute of Macromolecular Chemistry, Academy of Sciences of the Czech Republic, 162 06 Prague, Czech Republic
[2]Institute for Polymer Research, 01069 Dresden, Germany

Summary: The molecular and supermolecular orientation, morphology and structural changes observed during cold drawing of injection moulded isotactic polypropylene modified by specific α, and β nucleating agents were studied by polarised photoacoustic FTIR spectroscopy, wide-angle X-ray diffraction and differential scanning calorimetry. Significantly lower molecular orientation was found in the core of the β-nucleated injection moulded specimens as compared to unmodified and α-nucleated materials. This has been ascribed to the fast growth of the β-crystallites which inevitably dislocates the flow-induced orientation within the crystalline regions and in their vicinity. Moreover, it was found that the presence of the developed β-crystallites distinctly diminishes the efficiency of the orientational solid-state drawing assessed on both levels of the hierarchical structure (molecular and crystalline). This structural observation is directly connected with macroscopic softening effect of the β-phase: lowering the yield stress and flattening the neck shoulder. Thus, the interrelation between the microstructural and macroscopic effects of the β-phase could be described as a feedback process.

1 Introduction

Isotactic polypropylene has an important position among commodity polymeric materials. Despite its chemical simplicity it shows a remarkable complexity of crystal structures[1]. Attention has been paid especially to its α and β modifications. Both modifications are normally observed in real polypropylene parts. Preceding observations have already proven that β-phase contained in polypropylene has a favourable effect on particular mechanical properties, namely drawability and toughness[2,3]. The content of β-phase in a bulk polypropylene can be increased by appropriate choice of processing conditions[1] (temperature, pressure or stress conditions), but the most effective way to influence the crystalline modifications and their content is to use specific nucleating agents[4].

The most common ways of processing thermoplastic polymers are injection moulding and extrusion. Polymer profiles after extrusion are often additionally drawn at

 CCC 1022-1360/00/$ 17.50+.50/0

temperatures below their melting temperature T_m. During the solid-state drawing dramatic changes of the polymer morphology occur thus markedly influencing the end-use properties of the materials.

The aim of this work is to investigate the effects of specific nucleating agents on the molecular and supermolecular orientation of injection-moulded polypropylene and to monitor the changes in orientation during cold drawing. Attention has been paid also to the skin-core effect, which is characteristic for injection moulded parts. The combination of several structure-sensitive methods (WAXS, PPA FTIR, DSC) allowed to characterise the structural transformations and changes in orientation on molecular and supermolecular levels of the α- and β-nucleated polypropylene.

2 Experimental

2.1 Materials

The starting material used in this study was isotactic polypropylene Mosten 58.412 supplied by CHEMOPETROL Litvínov, Czech Republic. The manufacturer characterises the material by the melt flow index of 3 g/10 min (21.2 N, 230 °C) and the weight-average molecular weight M_w of about 170, 000.

The master batches of the specific nucleating agents were at first prepared by premixing nucleating agents in a *Brabender Plasticorder* with a small quantity of polypropylene. The characteristics of the nucleating agents are summarised in Table 1.

Table 1. Specific nucleating agents used in this work.

Nucleating agent (code)	Commercial name	Chemical nature
α^1	Millard 3988	based on sorbitol
α^2	ADK NA-11	on phosphorous base
β	NJ Star NU 100	*N',N'*-dicyclohexylnaphthalene-2,6-dicarboxamide

The master batches of the nucleating agents were then mixed with pellets of isotactic polypropylene in a ZE25-CL mixer in defined concentrations. Standard dumbbell specimens (DIN 53 455) were prepared by injection moulding in an extruder BATTENFELD BA 500 CD PLUS. The injection-moulding conditions are summarised

in Table 2a. The code and material composition can be seen in Table 2b.

Table 2a. The injection-moulding conditions.

Heating zone temperatures	220, 230, 240, 230 and 220 °C
Die temperature	240 °C
Mould temperature	60 °C
Screen compression ratio	2.2
Screw back pressure	5 bar
Injection pressure	620 bar
Holding pressure	620 bar
Holding pressure time	60 s
Freezing time	30 s
Cycle time	120 s

Table 2b. Characterisation of the PP samples.

Code	Composition
PP	PP (neat)
$PP\beta_{min}$	PP + 0.03 % β
$PP\beta_{max}$	PP + 0.1 % β
$PP\alpha^1$	PP + 1 % α^1
$PP\alpha^2$	PP + 1 % α^2

2.2 Specimen preparation and drawing

Injection-moulded dumbbell specimens were used for tensile testing and structural characterisation. Some of the specimens were subsequently drawn in a temperature chamber of Zwick 1456 Tensile Tester at 100 °C and drawing speed of 20 $mm.min^{-1}$. Equidistant marks (5 mm distance) were marked at the surface of the gauge length to assess the local drawing ratio λ of the drawn specimens. The specimens were fixed in the grips of the tensile tester and left 30 min in the closed temperature chamber at 100 °C before the test started. After the test the specimens were kept for a further 30 min in the grips to relax in the chamber at the same temperature and only then slowly cooled to room temperature in opened chamber. The chamber dimensions allowed the material to be drawn to the maximal elongation of $\Delta l = 200$ mm ($\varepsilon_{max} = 2$).

2.3 Techniques for structure characterisation

Wide-angle X-ray scattering

A diffractometer P4 (BRUKER-AXS) using Cu-K_α radiation (monochromatised by primary graphite crystal) was used for the WAXS analysis of all studied materials. The diffractometer measured the radial scattering range: $2\theta = 1.5 \ldots 40.5°$ in transmission by area detection system HiStar / GADDS. Diameter of the detector pinhole was 0.5 mm (distance 12 cm), measuring time $\Delta t = 180$ s (accumulation). The standard 2-dimensional scattering patterns were obtained and subsequently evaluated.

The overall crystallinity X_c, relative amount f_β of the β-phase and orientation of both α and β crystalline phases were evaluated from the surface (skin) and inner (core) regions of the injection moulded and subsequently drawn specimens. To measure the skin and core separately, layers with a thickness of 0.5 mm (for skin) and 1 mm (for core) were carefully cut by a razor blade. Drawn samples were cleaved in liquid nitrogen. The azimuthal intensity distribution for α and β reflections and X-ray diffraction pattern for crystallinity assessment for each sample were obtained by integration procedure from Debye-Scherrer diagrams as shown in Fig. 1a,b.

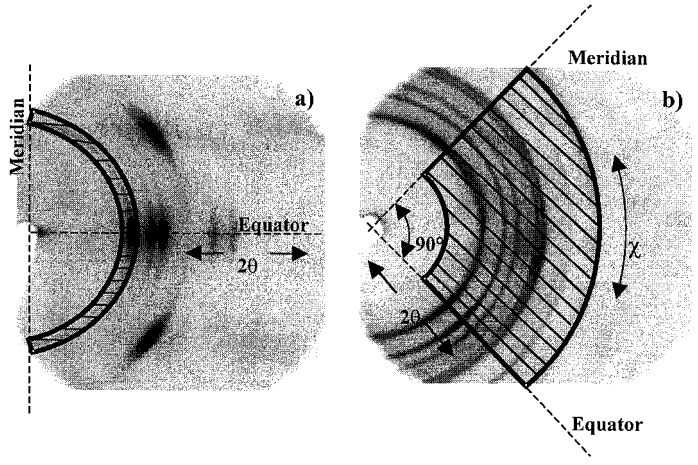

Fig. 1. Schematic representation of intensity integration from Debye-Scherrer diagrams (α^1-nucleated polypropylene): a) integrated intensity for assessment of azimuthal intensity distribution (drawn material) b) integrated intensity for crystallinity assessment (injection moulded material).

All studied materials show quadrant symmetry. The integration of one quadrant area is

therefore sufficient approximation for the crystallinity assessment. The relative amount f_β of the β-phase in the crystalline part of the specimens was evaluated from diffraction patterns by using the method of Turner-Jones et al.[5]:

$$f_\beta = \frac{I_\beta}{I_{\alpha 1} + I_{\alpha 2} + I_{\alpha 3} + I_\beta} \quad (1)$$

where I_β is the integral intensity of (300) reflection of the β-phase, and $I_{\alpha 1}$, $I_{\alpha 2}$, and $I_{\alpha 3}$ are the integral intensities of the (110), (040), and (130) reflections, respectively.

Full-width at half maximum (*FWHM*) was taken as a suitable characteristic of the crystalline phase orientation. The degree of orientation was characterised by the relative orientation parameter O_{rel} :

$$O_{rel} = \frac{180° - FWHM}{180°} \in (0;1) \quad (2)$$

Differential scanning calorimetry

DSC thermograms were measured by a *Perkin-Elmer DSC 7* (*Pyris* software version 3.51) over the temperature range 10 - 210 °C at a heating rate of 10 $Kmin^{-1}$ (and also 20, 40 and 80 $Kmin^{-1}$ for β-nucleated materials). The thermograms were obtained from the same specimens cut out from the surface and core regions as for the WAXS measurements. The enthalpy of fusion ΔH_f can be used as a second quantitative assessment of crystallinity assuming that the enthalpy of fusion $\Delta H_f°$ of both 100 % crystalline α- and β-phase is approximately the same ($\Delta H_f° \approx 191.3$ Jg^{-1}, after Wunderlich[6]). The crystallinity index X_c (mass fraction) can be written as:

$$X_c = \frac{\Delta H_f}{\Delta H_f°} \quad (3)$$

where ΔH_f is the total enthalpy of fusion of the specimen. Using the same assumptions, the relative proportion of the β-phase can be calculated by using the relationship[7]:

$$f_\beta = \frac{\Delta H_\beta}{\Delta H_f} \quad (4)$$

where ΔH_β is the enthalpy of fusion of the β-phase.

IR spectroscopy

Polarised photoacoustic Fourier-transform infrared (PPA FTIR) measurements were performed with an infrared spectrometer Bruker IFS66v/S using an MTEC 200

photoacoustic cell, Ames, IW). Experimental and theoretical details of this technique have already been published[8,9]. Injection moulded specimens were measured at the surface and also in the core region. The sampling was performed from the central part of the dumbbell specimens as shown in Fig. 2a. The specimens were cleaved by a special knife immediately after removing from liquid nitrogen. This allowed to measure the core region of a specimen without damaging its inner morphology. The cleaving direction was parallel to the axis of the dumbbell specimen (see Fig. 2). The specimen dimensions were in this case 8×5×4 mm^3.

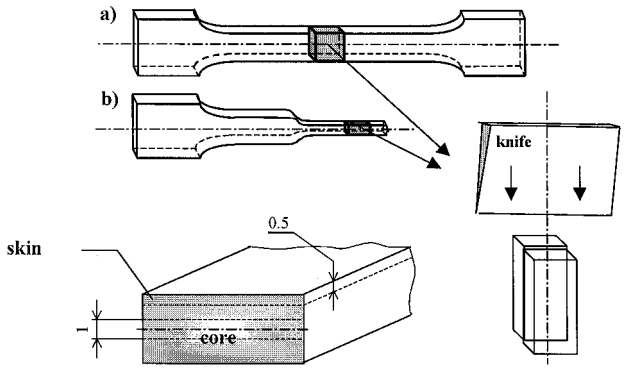

Fig. 2. Sample preparation: a) injection-moulded specimen, b) drawn specimen.

Specimens of the drawn materials were taken from the neck region as shown in Fig. 2b. Cleaving direction was parallel to the draw direction. Dimensions of the cleaved specimens were in this case 8×4×~1.5 mm^3.

After the cell holder with the specimen was inserted into the spectrometer, the cell was flushed with He for 1 h before the beginning of the measurement. The carbon-black standard was used as a reference and the resolution was 4 cm^{-1}. The infrared spectra were measured with mirror frequency of 2.2 kHz, 1000 scans being accumulated. The direction of the specimen orientation coincided with the plane in which the infrared beam passed through the photoacoustic cell. A KRS-5 wire grid polariser (SPECAC) was placed immediately in front of the cell. Two successive measurements, with parallel (||) and with perpendicular ($\perp$) polarisation of the electric vector with respect to the draw direction of the specimen, were used. The infrared dichroism[10] of two

characteristic polypropylene bands 998 cm^{-1} and 973 cm^{-1} was used as a parameter of molecular orientation[11]. Monochromatic infrared dichroism was at first determined by the relation $D = I_0/I_{90}$, where I_0 is the intensity of the photoacoustic signal of the corresponding band measured with polariser parallel and I_{90} the intensity with polariser perpendicular, respectively. A simplified relation for the orientation function:

$$f_{PAS} = \frac{(D-1)}{(D+2)} \tag{5}$$

was then used as characteristic of molecular orientation.

Light polarising microscopy

An optical microscope ZETOPAN fitted with crossed polariser and digital camera COHU was used for the characterisation of β-spherulites in injection moulded specimens. The thin sections were prepared by means of a microtome and then directly observed in transmitting light.

3 Results and discussion

3.1 Injection moulded materials

Overall crystallinity X_c of injection moulded specimens and the content of β-phase f_β assessed by DSC and WAXS measurements are reported in Table 3.

Table 3. Comparison of WAXS and DSC data for injection-moulded materials. The deviations of the real diffractograms from the fitted curves are also included.

Material	X_c [%]				f_β [%]			
	skin		core		skin		core	
	WAXS	DSC	WAXS	DSC	WAXS	DSC	WAXS	DSC
PP	56±5	52	59±4	53	0	0	0	0
$PP\beta_{min}$*	55±6	48	59±7	52	50±6	44	85±7	79
$PP\beta_{max}$*	58±7	49	61±7	52	76±7	59	89±7	83
$PP\alpha_1$	60±5	47	61±6	53	0	0	0	0
$PP\alpha_2$	56±6	48	59±6	53	0	0	0	0

* Crystallinities of the β-nucleated materials were assessed from the DSC thermograms measured at a heating rate of 40 $Kmin^{-1}$

The WAXS crystallinity determination was carried out using the peak area method in

the scattering range of 2θ = 10° – 30°. This method involves some difficulties in the amorphous-halo determination. As good approximation for all samples a maximum of amorphous halo at 2θ = 18° and a Gaussian profile were taken into account for fitting. The differences in crystallinity can be thus better estimated from enthalpy values assessed by DSC measurements.

It can be seen that nucleated specimens show differences in crystallinity between the skin and core regions. Obviously, this reflects the difference in the cooling rate between the skin and core regions. The surface of the specimens in direct contact with the mould wall was cooled very quickly, while the bulk of the sample was allowed to cool more slowly. Consequently, the nucleation process was also different in the skin and core regions. Neat polypropylene contained only α-spherulites with a broad size distribution. The addition of either of the two types of α-nucleating agents favourably improved the homogeneity of the spherulites especially in the core, as demonstrated also by the melting endotherms in Fig. 3a.

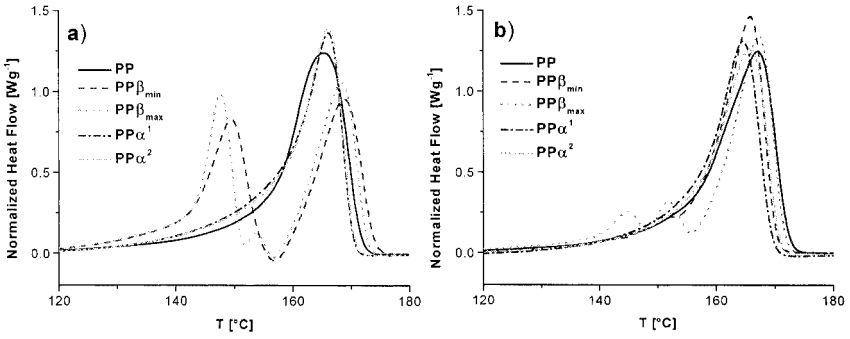

Fig. 3. Thermograms of polypropylene modified with different nucleating agents measured at heating rate of 10 $Kmin^{-1}$: a) core b) skin.

The DSC thermograms of both α-nucleated materials show no differences in melting behaviour in the core (Fig. 3a) and only a small difference in the melting temperature (2 K) at the skin (Fig. 3b). The addition of the β-nucleating agent also considerably enhanced the skin-core effect. The β-spherulites were for both concentrations (0.03 and 0.1 %) nucleated predominantly in the core regions (Fig. 3a), while at the surface β-nucleation was suppressed (Fig. 3b). Again, this can be explained by different cooling rates during the injection moulding process. From recent studies it is known[12] that the radial growth rate of the β-spherulites is higher for β-spherulites in the temperature

range of 100 to 140 °C with maximum approximately at 123 °C. In all cases the mould temperature was 60 °C and it is clear that under these conditions β-nucleation at the surface was restrained.

Two characteristic α and β peaks (148° and 168 °C, respectively) are shown in Fig. 3a,b for both β-nucleated materials. The small maximum at thermograms at 153.5 °C (see Fig. 3a,b) for sample with higher content of β-nucleating agent ($PP\beta_{max}$) is caused by the reorganisation process during the DSC experiment at the low heating rate of 10 $Kmin^{-1}$, as was also described by Kotek et al.[13]. This reorganisation process is demonstrated in Fig. 4, where thermograms measured at heating rates of 10, 20, 40 and 80 $Kmin^{-1}$ can be seen. At lower heating rates a β to α transformation occurs and that fact explains our decision to estimate the β-content f_β at the heating rate of 40 $Kmin^{-1}$ for both β-nucleated materials (see Table 3). The shape of the curve measured at 80 $Kmin^{-1}$ indicates a certain content of α-modification not formed during heating.

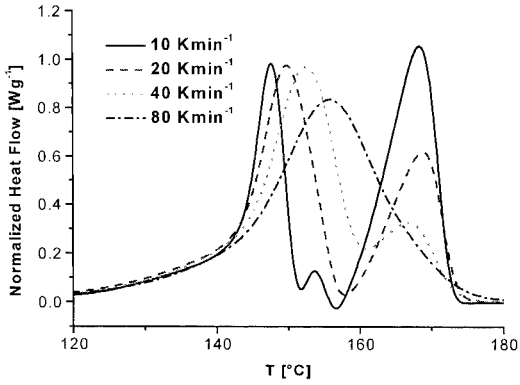

Fig. 4. The effect of the heating rate on reorganisation process of the β-nucleated material ($PP\beta_{max}$), core region.

The β-spherulites can be easily distinguished by light polarised microscopy under crossed polarisers with the same light intensity as can be seen for both concentrations in Fig. 5a,b.

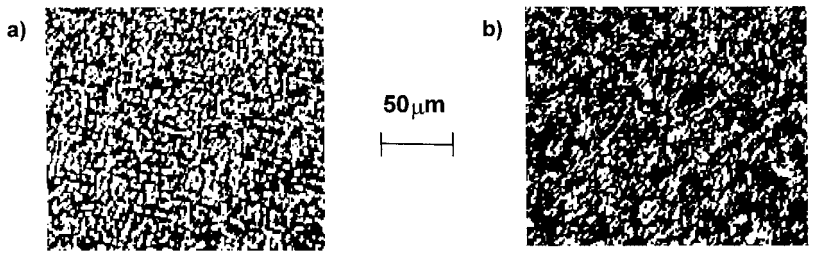

Fig. 5. The morphology of the core regions of polypropylene modified by β-nucleating agent at two different concentrations: a) 0.1 %, b) 0.03%. Light microscopy in polarised light.

Two different techniques were used for the description of the orientation process, namely wide angle X-ray scattering and polarised photoacoustic FTIR spectroscopy. Both techniques detect the orientation principally by different means. To characterise the molecular orientation in α-crystalline domains, the (040) reflection was observed in the diffractometer with the sample held normal to the primary beam axis (perpendicular to the dumbbell axis). The molecular orientation of the β-phase was assessed analogously from the (300) reflection. The azimuthal intensity distribution of the reflection was then fitted using a Lorenzian profile as the best approximation for narrow distribution. The *FWHM* values were then calculated from the width of distribution. The orientation degrees O_{rel} of injection-moulded materials are summarised in Table 4.

Table 4. The orientation characteristics of injection moulded samples.

Material	skin				core			
	O_{rel}		f_{PAS}^{973}	f_{PAS}^{997}	O_{rel}		f_{PAS}^{973}	f_{PAS}^{997}
PP	0.75		0.15	0.21	0.64		0.10	0.13
$PP\beta_{min}$	0.78	$0.69^{(\beta)}$	0.16	0.22	0.64	$0.57^{(\beta)}$	0.09	0.10
$PP\beta_{max}$	0.83	$0.74^{(\beta)}$	0.29	0.37	0.61*	$0.87^{(\beta)}$	0	0.04
$PP\alpha_1$	0.88		0.38	0.51	0.91		0.07	0.08
$PP\alpha_2$	0.90		0.33	0.51	0.89		0.07	0.10

* The O_{rel} calculated from (110) reflection
$^{(\beta)}$ The O_{rel} for β-modification calculated from (300) reflection

In all cases marked differences between the orientation at the skin and core regions of the specimens can be seen. The O_{rel} values are distinctly higher at the skin than in the core. Such differences could be ascribed to the different stress conditions in the mould

during injection moulding and subsequent crystallisation. Macromolecules are more oriented near the mould walls. During crystallisation the orientation is probably more or less disrupted depending on the crystallisation conditions. One exception is represented by the α^1-nucleated material, where the orientation of the α-crystalline domains is slightly higher in the core. Both types of the α-nucleated materials show very high orientation in the α-crystalline phase.

Moreover, the WAXS analysis allowed also to evaluate the O_{rel} values for β-crystalline phase by observing the [300] reflection. This reflection seems to be an overlapping of two kinds of β-phase with different quality of ordering. The more complicated behaviour in ordering and orientation of the β-phase can be expressed by the non-uniform azimuthal intensity distribution of the (300) reflection. Besides a maximum in the equatorial direction we find also a M-shaped distribution around the meridional direction (compare in Fig. 6).

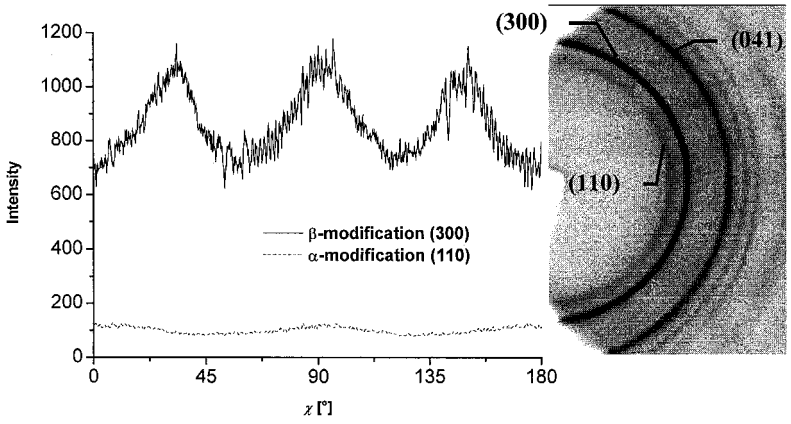

Fig. 6. Azimuthal intensity distribution of the α and β-reflections for β-modified material ($PP\beta_{max}$). Two-dimensional diffraction pattern can be seen on the left-hand side (equator = 90°).

Additionally, the ratio of the two detectable reflections (300) and (041) can be calculated to have different values dependent on the preparation conditions. Assuming a different role of the β-crystallites with maintained hexagonal lateral order, a marked influence on the (041) intensity can be expected, which is diminished for higher distortions, whereas the (300) intensity is kept constant. The orientation factor O_{rel} assessed for β-phase in Table 4 thus reflects only the orientation of a part of the overall

β-phase. In this case, the full width at half maximum was assessed from the maximum positioned in equatorial direction.

The simplified relations for orientation function f_{PAS} assessed by PPA FTIR spectroscopy reflect the molecular orientation of both amorphous and crystalline phases. All materials show higher values of orientation function at the skin than in the core, as observed for O_{rel} values. Orientation measured in the core of the specimens is very low especially for polypropylene with higher content of the β-nucleating agent (PPβ$_{max}$). The effect demonstrated in Fig. 6 plays also important role.

On the other hand, orientation measured by the two different methods in the skin coincides relatively well (the O_{rel} and f_{PAS} values are not comparable absolutely!). Again PPA FTIR measurements show highest values of orientation for α-nucleated materials. Orientation functions calculated from the so-called crystalline band f_{PAS}^{997} (band 997 cm^{-1}) show in all cases higher values then functions determined from the amorphous band f_{PAS}^{973} (band 973 cm^{-1}). This fact indicates that molecular orientation relating to direction of injection moulding is higher in crystalline domains than in the amorphous phase for all the injection moulded specimens, studied.

3.2 Drawn materials

Specimens prepared by injection moulding were subsequently drawn at 100 °C. This temperature was chosen in order to suppress the stress whitening, which complicates the WAXS data evaluation. This temperature is also very close to the optimum drawing temperature for polypropylene (110 °C) [14]. The average stress strain curves for each material are presented in Fig. 7. Each average curve was calculated from five individual measurements. Tensile mechanical characteristics derived from the curves are summarised in Table 5.

Table 5. Tensile mechanical properties for the injection-moulded specimens. $\sigma_{y,100}$ is yield stress and $\varepsilon_{y,100}$ yield strain at 100 °C and E_{23} or E_{100} are moduli of elasticity measured at 23°C or 100 °C, respectively.

Material	$\sigma_{y,100}$ [MPa]	$\varepsilon_{y,100}$ [%]	E_{23} [MPa]	E_{100} [MPa]
PP	10.9±0.1	10.5±0.2	1557±95	520.2±69
PPβ$_{min}$	9.4±0.1	9.7±0.3	1398±38	534.4±25
PPβ$_{max}$	9.8±0.2	7.6±0.1	1481±97	593.1±38
PPα$_1$	12.9±0.1	9.5±0.1	1971±73	704.5±23
PPα$_2$	14.5±0.3	7.5±0.2	2094±86	692.1±48

All materials exhibit a yield stress (measured at the peak position) and inhomogeneous drawing by neck propagation. Stress whitening appears during tensile testing of all specimens. The α^2-nucleated material and material with a higher content of the β-phase exhibit a more extensive stress whitening. This is probably connected with the different spherulite size distributions in the individual materials and also with the level of the overall crystallinity. The α^2-modified material exhibits the highest value of the yield stress followed by the material modified by α^1-nucleating agent. The yield stress values of both β-modified materials are lower then the corresponding values of the α-nucleated and neat materials. It should be also noted that the stress level during the solid-state drawing of the β-nucleated material is also much lower than the corresponding values for the neat and α-nucleated materials. Lower energy consumption during the tensile deformation of the β-nucleated materials is accompanied by the flattening of the neck shoulder as demonstrated in Fig. 7. The macroscopic neck geometry, in turn, controls the intensity of the structural transformation at microscopic dimensions. Thus, a feedback process could be described between the molecular and macroscopic deformation mechanisms.

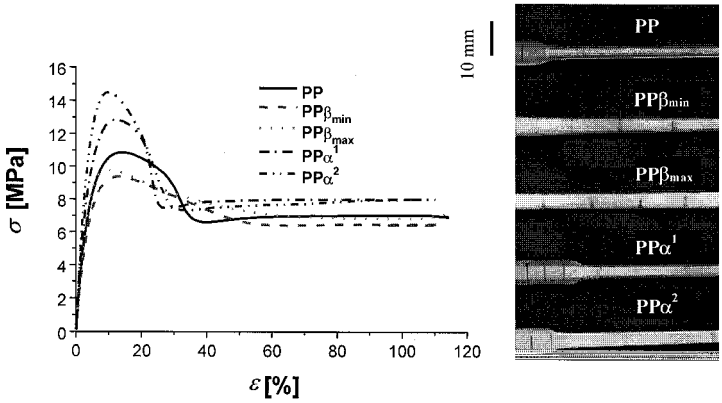

Fig. 7. Stress-strain curves of materials based on polypropylene. The effect of the specific β-nucleation is demonstrated on the left-hand side.

Structural parameters were assessed for the skin and core portions separately for all drawn specimens. The results are summarised in Table 6, together with the values of the natural drawing ratio λ (maximal obtained during one-step drawing at given conditions). It is shown that the overall crystallinity is increased significantly for all studied specimens upon drawing. The differences between skin and core are within the

experimental error. The content of the β-phase f_β could be detected by WAXS only.

Table 6. Comparison of WAXS and DSC data for drawn materials.

Material	λ	X_c [%]				f_β [%]			
		skin		core		skin		core	
		WAXS	DSC	WAXS	DSC	WAXS	DSC	WAXS	DSC
PP	5.0	61±5	55	63±5	55	0	0	0	0
$PP\beta_{min}$	4.6	61±6	55	62±5	55	6±6	-	17±5	-
$PP\beta_{max}$	4.0	59±5	55	62±4	55	10±5	-	18±4	-
$PP\alpha_1$	5.1	59±7	55	60±6	54	0	0	0	0
$PP\alpha_2$	5.1	60±4	56	63±5	54	0	0	0	0

In Fig. 8 can be seen the melting endotherms of all the materials studied. Neat polypropylene exhibits two melting peaks (T_{m1}= 162 °C, T_{m2} =171 °C) observed in both the core and skin regions. This reflects the coexistence of two different crystalline structures. The peak detected at 162 °C is suppressed in all nucleated materials (especially for both β-nucleated materials in the core). In the core region that peak almost vanishes.

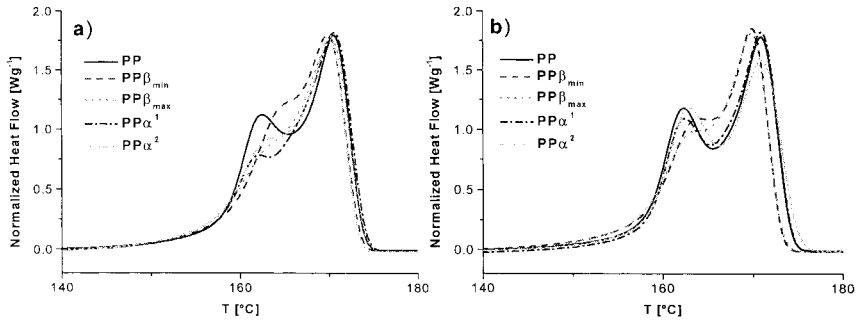

Fig. 8. Melting endotherms of all drawn materials: a) core b) skin

The orientation of the studied materials was evaluated by the same procedure as that used for injection moulded specimens. One exception is the assessment of O_{rel} values, which were calculated from the reflection (110) because of overlapping of the (040) reflection by the β-reflection (300) in β-nucleated materials. The orientation degrees O_{rel} of drawn materials are summarised in Table 7.

Table 7. The orientation characteristics of drawn samples.

Material	λ	skin				core			
		O_{rel}		f_{PAS}^{973}	f_{PAS}^{997}	O_{rel}		f_{PAS}^{973}	f_{PAS}^{997}
PP	5.0	0.947		0.70	0.88	0.944		0.57	0.74
$PP\beta_{min}$	4.6	0.921	*	0.69	0.89	0.899	*	0.57	0.73
$PP\beta_{max}$	4.0	0.914	0.801^{β}	0.69	0.93	0.915	0.779^{β}	0.62	0.74
$PP\alpha_1$	5.1	0.951		0.73	0.90	0.944		0.61	0.73
$PP\alpha_2$	5.1	0.944		0.81	0.95	0.933		0.71	0.75

* The assessment of the O_{rel} was precluded because of overlapping of both α and β-reflections

The skin again shows again higher O_{rel} values then the core in all studied materials. The highest values of orientation can be seen for neat and α^1-nucleated materials. Lower O_{rel} values were detected in the crystalline phase of both β-nucleated materials. The β-phase is gradually transformed to α-phase. That effect is related to the lower drawing ratios obtained here. X-ray diffraction analysis allowed to assess O_{rel} of the β-phase for the sample with higher β-phase content ($PP\beta_{max}$). The orientation of that "residual" β-phase is very low compared with α-phase and is changed by drawing only slightly (see Fig. 9).

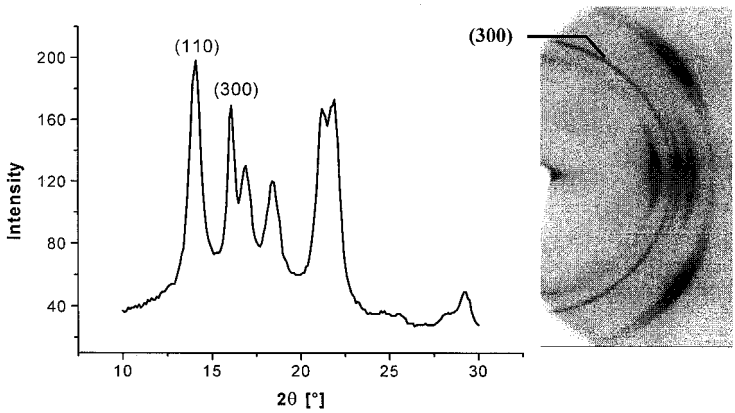

Fig. 9. Two and one dimensional X-ray diffraction pattern for drawn β-nucleated material, λ = 4.0, ($PP\beta_{max}$).

A similar effect was observed also for the sample with lower content of β-phase ($PP\beta_{min}$). Unfortunately, in this case numerical assessment of the O_{rel} was precluded because of overlapping of both α and β-reflections.

The simplified relations for orientation functions f_{PAS} again show higher values at the

skin than in the core, similar to the O_{rel} values. Nevertheless, the f_{PAS} values do not show marked differences between the α- and β-modified materials.

4 Conclusions

The modification of isotactic polypropylene by different kinds of nucleating agents considerably influences the morphology on both the molecular and supermolecular levels. Moreover, nucleation changes the drawing behaviour and the resulting orientation. Significantly lower molecular orientation was found in the core of the β-nucleated specimens as compared to unmodified and α-nucleated materials. This might be ascribed to the fast growth of the β-crystallites which inevitably dislocates the flow-induced orientation within the crystalline regions and in their vicinity.

Moreover, it was found that the presence of the developed β-crystallites distinctly diminishes the efficiency of the orientational solid-state drawing as measured by the development of orientation both on levels of the hierarchical structure (molecular and crystalline). β-phase is gradually transformed to α-phase. Nevertheless, the orientation of residual β-phase is changed only slightly during the solid-state drawing. This structural observation is directly connected with a macroscopic softening effect of the β-phase: lowering the yield stress and flattening the neck shoulder. Thus, the interrelation between the microstructural and macroscopic effects of the β-phase could be described as a feedback process.

Acknowledgements

One of the authors (J.Š.) was sponsored by the Saxonian Government during his stay at the Institute for Polymer Research Dresden (project SMWK-Az. 4-7531.50-04-821-00/7). The support of the Grant Agency of the Academy of Science of the Czech Republic (project A4050904 and 106/02/1249) is also gratefully acknowledged. We are also indebted to Processing Department of the Institute for Polymer Research Dresden for technical support in the sample preparation and to Dr. L. Pospíšil, Polymer Institute Brno, for providing the nucleating agents. Thanks are also given to Dr. G. Pompe, IPF Dresden, for her helpful discussion of the DSC results, to D. Beyerlein MSc. for making the photographs and Mrs G. Adam, IPF Dresden, for very helpful technical assistance.

References

[1] M. Aboufaraj, B. Ulrich, A. Dahoun, C. G´Sell, *Polymer*, 1993, **34**, 4817.
[2] S. C. Tjong, J. S. Shen, R. K. Y. Li, *Polym. Eng. Sci.*, 1996, **36**, 100.
[3] M. Raab, J. Kotek, J. Baldrian, W. Grellman, *J. Appl. Polym. Sci.*, 1998, **69**, 2255.
[4] A. Galeski, *Nucleation of Polypropylene* in J. Karger-Kocsis. *Polypropylene Structure, Blends and Composites*, Vol. 1 *Structure and Morphology*, Chapman&Hall, London, 1995, pp.131.
[5] A. Turner-Jones, J. M. Aizelwood, D. R. Beckett, *Macromol. Chem.* 1964, **75**, 134.
[6] B. Wunderlich, *Macromol. Phys.*, 1980, **3**, 63.
[7] J. X. Li, W. L. Cheung, *J. Vinyl & Additive Tech.*, 1997, **3**, 151.
[8] P. Schmidt, M. Raab, J. Kolarik, K.-J. Eichhorn, *Polym. Test.*, 2000, **19**, 205.
[9] K.-J. Eichhorn, I. Hopfe, P. Pötschke, P. Schmidt, *J. Appl. Polym. Sci.*, 2000, **75**, 1194.
[10] T. Miyazawa, *J. Polym. Sci. C*, 1964, **7**, 59.
[11] P. Schmidt, J. Baldrian, J. Ščudla, J. Dybal, M. Raab, K.-J. Eichhorn, *Polymer*, 2001, **42**, 5321.
[12] Ph. Tordjeman, C. Robert, G. Marin, P. Gerard, *Eur. Phys. J. E*, 2001, **4**, 459.
[13] J. Kotek, J. Kratochvíl, J. Baldrian and M. Raab, *Macromol. Symposia*, in press.
[14] A. J. Wills, G. Cappacio, I. M. Ward, *J. Polym. Sci.*, 1980, **18**, 493.